Eur Radiol (2005) 15: 864–871
DOI 10.1007/s00330-005-2672-6

CARDIAC

Konstantin Nikolaou
Javier Sanz
Michael Poon
Bernd J. Wintersperger
Bernd Ohnesorge
Teresa Rius
Zahi A. Fayad
Maximilian F. Reiser
Christoph R. Becker

Assessment of myocardial perfusion and viability from routine contrast-enhanced 16-detector-row computed tomography of the heart: preliminary results

Received: 25 October 2004
Revised: 6 January 2005
Accepted: 11 January 2005
Published online: 18 March 2005

Dr. Sanz's work is supported in part by a Research Grant ("Beca para la Formación en Investigación Post-Residencia") from the Spanish Society of Cardiology.

K. Nikolaou (✉) ·
B. J. Wintersperger · M. F. Reiser ·
C. R. Becker
Department of Clinical Radiology,
Ludwig-Maximilians-
University of Munich,
Munich, Germany
e-mail: konstantin.nikolaou@med.
uni-muenchen.de
Tel.: +49-89-70953620
Fax: +49-89-70958832

K. Nikolaou · J. Sanz · M. Poon ·
T. Rius
Zena and Michael A. Wiener
Cardiovascular Institute,
Mount Sinai School of Medicine,
New York, NY, USA

K. Nikolaou · Z. A. Fayad
Departments of Radiology and
Cardiology, Imaging Science
Laboratories, Mount Sinai
School of Medicine,
New York, NY, USA

M. Poon
Department of Cardiology,
Cabrini Medical Center,
New York, NY, USA

B. Ohnesorge
Siemens Medical Solutions,
Forchheim, Germany

Abstract To assess the diagnostic accuracy of 16-detector-row computed tomography (16DCT) of the heart in the assessment of myocardial perfusion and viability in comparison to stress perfusion magnetic resonance imaging (SP-MRI) and delayed-enhancement magnetic resonance imaging (DE-MRI). A number of 30 patients underwent both 16DCT and MRI of the heart. Contrast-enhanced 16DCT data sets were reviewed for areas of myocardium with reduced attenuation. Both CT and MRI data were examined by independent reviewers for the presence of myocardial perfusion defects or myocardial infarctions (MI). Volumetric analysis of the hypoperfusion areas in CT and the infarct sizes in DE-MRI were performed. According to MRI, myocardial infarctions were detected in 11 of 30 cases, and perfusion defects not corresponding to an MI were detected in six of 30 patients. CTA was able to detect ten of 11 MI correctly (sensitivity 91%, specificity 79%, accuracy 83%), and detected three of six hypoperfusions correctly (sensitivity 50%, specificity 92%, accuracy 79%). Assessing the volume of perfusion defects correlating to history of MI on the CT images, a systematic underestimation of the true infarct size as compared to the results of DE-MRI was found ($P<0.01$). Routine, contrast-enhanced 16-detector row CT of the heart can detect chronic myocardial infarctions in the majority of cases, but ischemic perfusion defects are not reliably detected under resting conditions.

Keywords Multidetector-row computed tomography · Magnetic resonance imaging · Myocardial perfusion · Myocardial infarction · Myocardial viability

Introduction

The reliable diagnosis of myocardial perfusion defects and myocardial infarction (MI) is of great interest in the comprehensive workup of coronary artery disease (CAD). The detailed assessment of myocardial perfusion defects can be crucial in the evaluation of the functional or hemodynamic impact of a given coronary artery lesion [1]. It has also been shown that the occurrence of an MI, even if it is asymptomatic, is associated with an increased risk of future ischemic events and an increased cardiac mortality [2]. A diagnostic tool that can provide detailed information on myocardial perfusion and viability at the same time not only will help in the prognostic assessment of the patient but will also be valuable in choosing appropriate therapeutic strategies (e.g. catheter revascularization).

In recent years, magnetic resonance imaging (MRI) has been tested extensively for the combined non-invasive assessment of myocardial perfusion, function and viability [3]. Differentiation of viable versus non-viable myocardium using delayed-enhancement magnetic resonance imaging (DE-MRI) techniques has been validated and can be considered as the reference standard for the detailed assessment of myocardial viability [4]. Stress-perfusion magnetic resonance imaging (SP-MRI), using adenosine as the stressing agent, has been reported to yield a high sensitivity and specificity in the detection of significant coronary artery lesions as compared to invasive cardiac catheterization [5, 6].

In addition, multidetector-row computed tomography (MDCT) has been validated as a useful non-invasive diagnostic method in patients with various cardiac diseases. Because of the combination of fast rotation time and multislice acquisition with a high spatial resolution, MDCT is able to provide detailed information on cardiac morphology and on the coronary arteries at the same time [7]. First systematic studies have shown the potential of this technique to detect and assess myocardial infarctions [8]. However, performing the routine 16-detector-row CT angiography (16DCTA) protocol of the heart and coronary arteries, areas of decreased CT attenuation can correspond to perfusion defects and/or infarcted tissue at the same time. In a number of cases, a clear differentiation of these two diagnoses is not possible using this technique.

Therefore, the purpose of this work was to correlate the MDCT findings to DE-MRI and SP-MRI as the reference standards for imaging of myocardial infarction and myocardial perfusion defects. This way, the value of routine, contrast-enhanced MDCT imaging of the heart for the detection of both of these pathological entities could be evaluated.

Materials and methods

Patient population

Thirty patients who had undergone cardiac 16DCTA, DE-MRI and SP-MRI between November 2002 and June 2003 were retrospectively identified. The mean time interval between MDCT and MRI was 10±16 days. The patients were evaluated in the Clinical Cardiac MR/CT Program in Mount Sinai Hospital (New York) for known or suspected CAD. The study was approved by the Internal Review Board of the institution. All subjects were >18 years old and signed a written informed consent. The patient population was characterized as follows: 22 males, eight females, mean age 63± 11 years (range 33–85 years). Indication for cardiac CTA and MRI was known (n=18) or suspected CAD (n=12). In all patients with history of prior myocardial infarction (MI) (n=11), the infarction was chronic (>3 months). The diagnosis of chronic myocardial infarction was based on the following criteria. Chronic MI was diagnosed if the patient had (1) a history of previous myocardial infarction, (2) diagnostic Q waves on the electrocardiogram or ECG registration of the acute event, and (3) normal enzyme levels during the observation period.

MDCT imaging protocol

All investigations were performed on a 16 detector-row CT scanner (Somatom Sensation 16; Siemens Medical Solutions, Forchheim, Germany). For contrast-enhanced MDCT of the heart, the following parameters were employed: 12×0.75 mm collimation, 0.42 s rotation time, temporal resolution of 105–210 ms, 120 kV, and 500 mA s, resulting in a total scan time of about 20 s to cover the entire heart acquired during suspended breathing using retrospective ECG gating. The contrast agent (100 cm^3 of ioversol; Optiray 320; Mallinckrodt Inc., St Louis, MO, USA) was infused at 3.5 ml/s followed by 50 ml of saline at the same rate, using a dual injector (Stellant; Medrad Inc., Indianola, Pa., USA). An automatic bolus-tracking system (CARE Bolus; Siemens Medical Solutions) was employed to trigger data acquisition 6 s after the attenuation of the aortic root reached a threshold of 100 Hounsfield units (HU). The data sets were reconstructed at mid- to end-diastole for optimal image quality, with a 1.0-mm slice thickness, using 0.5-mm increments. Thus, spatial resolution of the reconstructed images was 0.6×0.6×1.0 mm. The protocol as described here and used in this study is optimized for non-invasive coronary angiography, and this was the primary indication for the CT examinations.

MRI imaging protocols

For all MRI examinations, a 1.5 T system (MAGNETOM Sonata; Siemens Medical Solutions, Erlangen, Germany) was employed. Studies were performed with the patients lying in supine position, using a phased-array surface coil as a receiver and ECG gating.

Stress-perfusion MRI (SP-MRI)

Three short-axis sections were chosen for perfusion imaging with an electrocardiographically triggered T1-weighted saturation-recovery true-FISP sequence: repetition time (ms)/echo time (ms)/inversion time (ms) 634/0.86/84, flip angle 8°, FOV 285×380 mm^2, matrix 72×128, imaging time approximately 9 s, section thickness 10 mm, bandwidth 1370 Hz/pixel. The locations of the three sections were at the base, at the level of the midpapillary muscles, and at the apex. During an expiratory breath hold, a bolus of Gd-DTPA (Magnevist; Berlex, New Jersey, USA), 0.05 mmol/kg body weight, was injected at 5 ml/s and flushed with 20 ml of normal saline by using a power injector (Spectris; Medrad, Indianola, Pa., USA). During the first pass of the contrast agent, 60–80 dynamic images were acquired simultaneously at each of the three levels. Patients were instructed to hold their breath as long as possible and to start breathing gently when necessary. Stress perfusion was performed initially, using a continuous infusion of adenosine (Adenoscan; Sanofi Winthrop Industries, Notre Dame De Bondeville, France) at a rate of 140 μg/kg per minute. During the adenosine infusion, the patient's heart rate was monitored continuously with the physiologic monitor of the imager. Blood pressure measurements were obtained at the beginning and end of the infusion, and visual and verbal contact with the patient was maintained throughout the whole examination. The first set of dynamic perfusion images was acquired after 3 min of adenosine infusion. Approximately 15 min later (to allow for wash-out of the contrast agent), a second set of rest perfusion images was acquired using the same protocol as described above. After the second series of perfusion images was completed, another bolus of gadopentetate dimeglumine, 0.1 mmol/kg, was injected, i.e. the complete amount of contrast agent injected added up to 0.2 mmol/kg.

Delayed-enhancement MRI (DE-MRI)

Ten to 15 min after the administration of the first contrast bolus for perfusion imaging, short-axis images were acquired to assess the presence of delayed myocardial enhancement. For this purpose, a phase-sensitive inversion recovery-prepared gradient echo sequence was employed [9]. Contiguous LV short-axis views and one long-axis (four-chamber) view were obtained using the following imaging parameters: repetition time (ms)/echo time (ms)/inversion time (ms) 8.4/4.2/250, flip angle 25°, FOV 340×275 mm^2, matrix 256×128, imaging time approximately 9 s, slice thickness 8 mm, averages 1, gating factor 2, bandwidth 130 Hz/pixel.

Image analysis

The MDCT and MRI images were read by two independent reviewers with extensive experience in cardiac MDCT and MRI, blinded to all other clinical data or imaging data available. Both the MDCT and the MRI images were analyzed on a dedicated workstation (Leonardo; Siemens Medical Solutions). For all perfusion defects or myocardial infarctions detected on either the MRI or MDCT images, the reviewers had to allocate the myocardial area affected to one of the three following vascular supply territories: left anterior descending (LAD) territory (anterior wall, septum, apex); left circumflex (LCX) territory (lateral wall, inferolateral wall); right coronary artery (RCA) territory (inferior wall, inferoseptal wall). Agreement in territory assignment between MRI and MDCT was graded as complete agreement (correct vessel territory and myocardial area), partial agreement (correct vessel territory but deviance in myocardial area), or no agreement.

The first-pass SP-MRI contrast-enhanced MR images were analyzed qualitatively for the presence or absence of regions of reduced contrast material uptake. Presence of hypo-enhancement in the vascular supply territories as described above was considered positive for perfusion defect and indicative of substantial stenosis affecting the corresponding coronary artery. For this evaluation, both information from rest and stress perfusion data was taken into account, and one final diagnosis (perfusion defect yes/no) had to be made from these two data sets by the MRI reviewer.

The DE-MRI short-axis images were analyzed for any hyper-enhancement from base to apex. Infarct size on each of these short-axis images was assessed quantitatively by manually contouring the hyper-enhanced area with use of the irregular region of interest on the console. The infarct size in each patient was then calculated as total infarct area multiplied by the section thickness.

Reviewing the MDCT images, areas of decreased myocardial attenuation constituted the basis for the diagnosis of a perfusion defect in this study, potentially corresponding to an MI or an ischemic perfusion defect caused by a significant coronary artery stenosis. The 2D-axial images and an interactive 3D multiplanar reformatted reconstruction (MPR) in short axis were used for analysis. The reader adjusted the windowing parameters visually on an individual basis. The typical window width and level settings ranged between 350–550 and 150–250 HU, respectively. The areas of decreased myocardial attenuation were manually traced on the short-axis images, to quantify the volume

of the hypo-perfused areas on MDCT, using the same method as with DE-MRI. Regions of interest of 0.5 cm^2 were placed in a non-infarcted segment and in a region with hypo-attenuation and the mean HU were recorded.

Statistical analysis

Categorical values are expressed as percentages and continuous variables as mean±SD. The sensitivity, specificity, and diagnostic accuracy for the detection of perfusion defects and/or MI in a per-patient basis were obtained. The *t*-test for the paired data was used to compare the MI volume measurements with each technique, as well as the attenuation difference between infarcted and non-infarcted segments. For statistical analysis, a commercially available Windows-based software product was used (SPSS 12.0.1, 2003).

Results

Results of MRI

Performing SP-MRI, perfusion defects were recorded in 17 cases. Nine of these perfusion defects were in the LAD territory, two in the LCX territory and six in the RCA territory.

The DE-MRI imaging revealed positive delayed hyperenhancement (DH) in all patients where history of prior myocardial infarction was positive. Thus, a total of 11 patients (37%) had a myocardial infarction as demonstrated by DE-MRI. The distribution according to vessel territories was as follows: LAD territory four cases, LCX territory two cases, and RCA territory five cases, respectively.

Comparing the perfusion defects and the myocardial infarctions as detected with SP-MRI and DE-MRI, all 11 infarctions as detected by DE-MRI also showed a perfusion defect in SP-MRI. Another six perfusion defects were detected by SP-MRI without signs of infarctions in DE-MRI, adding up to the total of 17 perfusion defects detected by SP-MRI as described above. These six perfusion defects not corresponding to a MI were true ischemic perfusion defects caused by a significant coronary artery stenosis. Five of these six ischemic perfusion defects were located in the LAD territory, and one perfusion defect was located in the RCA territory. In the six patients with perfusion defects in SP-MRI but no MI history, corresponding results of other tests showed typical ischemic ECG changes under stress conditions. Also, in all these six patients, significant coronary artery lesions in the main coronary arteries supplying the corresponding ischemic vessel territory were proven by conventional X-ray angiography.

MDCT versus SP-MRI for detection of perfusion defects

Comparing routine contrast-enhanced 16DCT of the heart with SP-MRI for the detection of perfusion defects, CTA was able to detect 13 of 17 hypoperfusion correctly, making one false-positive and four false-negative diagnoses (sensitivity 76%, specificity 92%, accuracy 83%). However, considering only the six perfusion defects not associated to a MI, sensitivity of MDCT at resting conditions for ischemic perfusion defects dropped to 50% (3/6 detected) (Table 1). All three perfusion defects missed in the LAD territory were located in the apex. Figure 1 shows an example of a perfusion defect in the RCA territory, positively detected by contrast-enhanced MDCT as compared to SP-MRI. In this case, no myocardial infarction was present according to the DE-MRI images.

MDCT versus DE-MRI for detection of myocardial infarctions

Comparing 16DCTA with DE-MRI for the detection of myocardial infarctions, CTA was able to detect ten of 11 infarctions correctly, making four false-positive and one false-negative diagnosis (sensitivity 91%, specificity 79%, accuracy 83%) (Table 1). The sensitivities for detection of myocardial infarctions according to the vascular supply territory were as follows: four of four perfusion defects in the LAD territory were detected (sensitivity 100%), two of

Table 1 Diagnostic accuracy of contrast-enhanced MDCT in comparison to stress-perfusion MRI (SP-MRI) and delayed-enhancement MRI (DE-MRI) in the detection of myocardial perfusion defects and myocardial infarctions, respectively. *LAD* left anterior descending coronary artery, *LCX* left circumflex coronary artery, *RCA* right coronary artery

MDCT vs SP-MRI				
	SP-MRI positive (*n* cases)	CT sensitivity (%)	CT specificity (%)	CT accuracy (%)
Overall	6	50	92	79
LAD territory	5	40		
LCX territory	0	n.a.		
RCA territory	1	100		
MDCT vs DE-MRI				
	DE-MRI positive (*n* cases)	CT sensitivity (%)	CT specificity (%)	CT accuracy (%)
Overall	11	91	79	83
LAD territory	4	100		
LCX territory	2	100		
RCA territory	5	80		

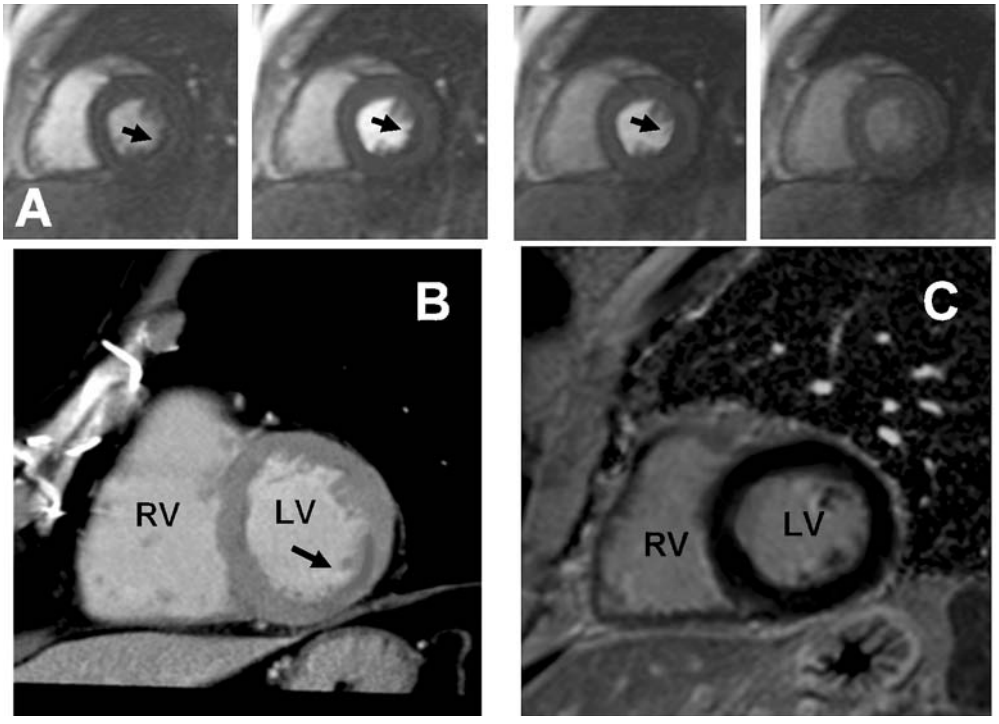

Fig. 1 Stress-perfusion magnetic resonance imaging (**a**), contrast-enhanced Multislice-CT (**b**) and delayed-enhancement MRI (**c**) in a 67-year-old male patient with chest pain. The perfusion MRI images prove presence of a subendocardial myocardial perfusion defect (**a**, *arrows*). Four exemplary perfusion phases are taken from the complete perfusion data set. Contrast-enhanced multislice CT also demonstrates an area of reduced myocardial attenuation likely due to reduced contrast uptake in this area of myocardium (**b**, *arrow*). However, delayed-enhancement MRI (**c**) excludes presence of a myocardial infarction, as there is no delayed contrast-enhancement in this area of myocardium. *LV* left ventricle, *RV* right ventricle

two defects in the LCX territory (100%), and four of five in the RCA territory (80%), respectively. Three out of four false-positive diagnoses were made in the LAD territory (apex and septum), and one false-positive diagnosis was made in the RCA territory (inferobasal). Figures 2 and 3 give examples of correctly identified myocardial infarction with MDCT as compared to DE-MRI.

Infarct volumetry and attenuation values

Retrospectively measuring the attenuation values (HU) in the ten infarcted areas detected correctly by MDCT, these attenuation values were significantly lower than in non-infarcted areas of myocardium (53.7±33.5 versus 122.3±25.5 HU; $P<0.01$). In the volumetric assessment of infarct size, a strong correlation between the volumes of 16DCT and DE-MRI was found ($r=0.98$), but 16DCT tended to underestimate the infarct volume as assessed by MRI by 19% ($P<0.01$) (Fig. 4). Mean infarct volumes in MDCT were 10.3±5.7 cm^3 (range 3.4–28.5 cm^3), compared to 12.4±7.2 cm^3 (range 2.7–21.8 cm^3) as measured in the DE-MRI images, respectively.

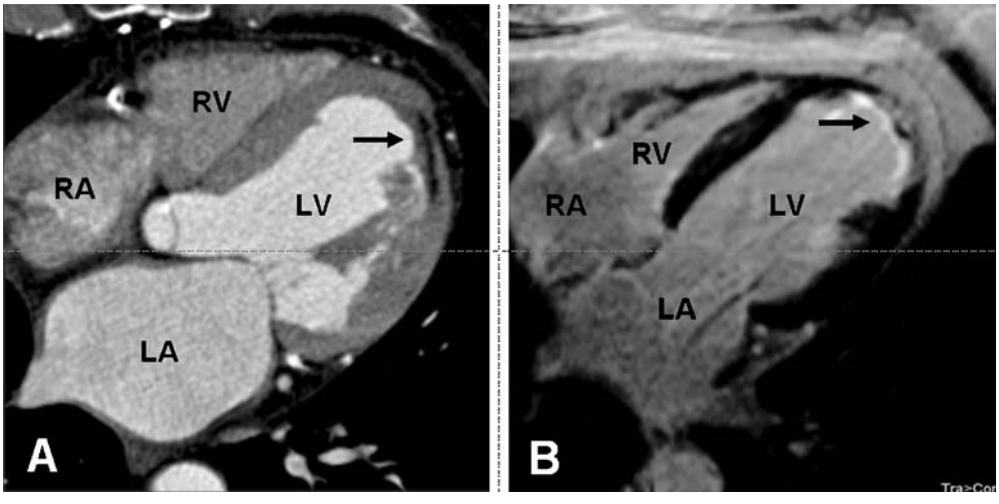

Fig. 2 Contrast-enhanced multislice CT (**a**) and delayed-enhancement MRI (**b**) of a 68-year-old male patient. In the contrast-enhanced MDCT images, an area of decreased attenuation is seen in the apical and anterior region of the left ventricular wall (**a**, *arrow*). In the same area of myocardium, a myocardial infarction is present, as proven by DE-MRI imaging (**b**, *arrow*). *LV* Left ventricle, *RV* right ventricle, *LA* left atrium, *RA* right atrium

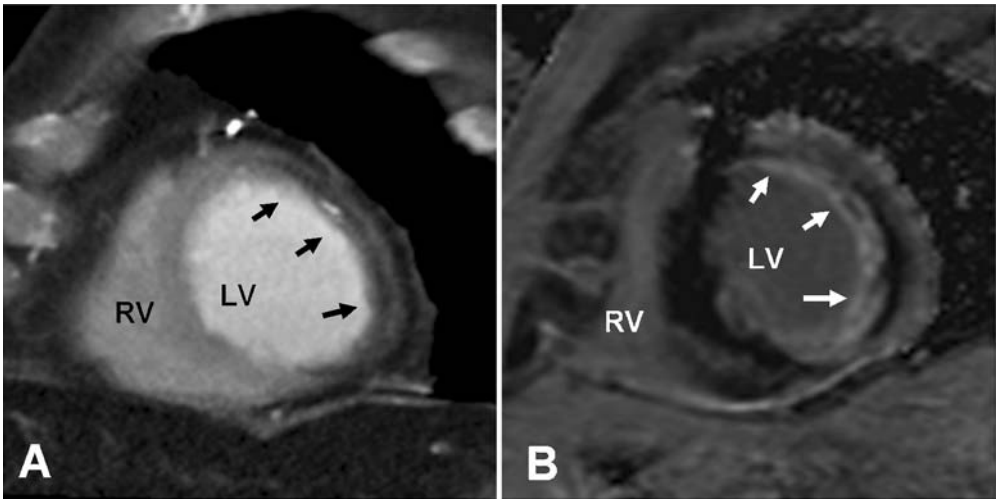

Fig. 3 Cross-sectional reconstruction of a contrast-enhanced multislice CT (**a**) compared to delayed-enhancement MRI (**b**) of an 85-year-old male patient. In the contrast-enhanced MDCT images, an extensive area of decreased attenuation is seen in the free lateral and parts of the basal wall of the left ventricle (**a**, *arrows*). In this area of myocardium, a large myocardial infarction is present, as proven my DE-MRI imaging (**b**, *arrows*). *LV* Left ventricle, *RV* right ventricle

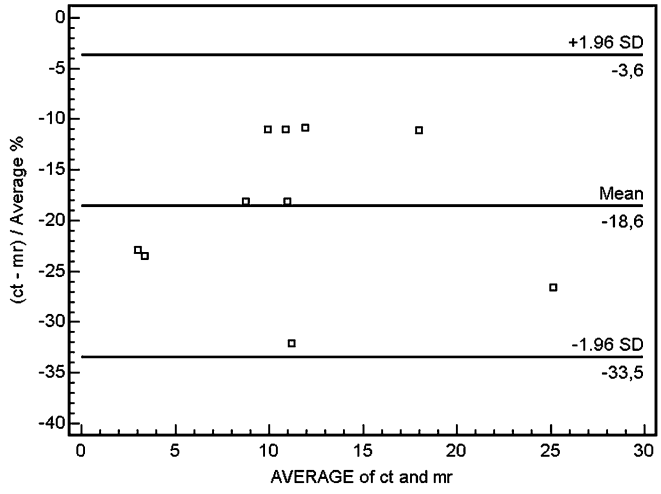

Fig. 4 Comparison of infarct volumes as assessed manually on the contrast-enhanced multislice CT and delayed-enhancement MRI, displayed as a Bland–Altman Plot. Infarct volumes show a good correlation, but a significant offset of about 19% of the volumes measured, i.e. MDCT significantly underestimates the true infarct volumes

Discussion

Detection of myocardial infarctions with MDCT

A number of early reports on the application of computed tomography (CT) in patients with myocardial infarction have been promising, including animal studies [10, 11] and experiences with electron beam CT [12, 13]; however, the clinical application of CT in the diagnosis of myocardial infarctions has not become popular thus far. With the introduction of multidetector-row computed tomography (MDCT) systems, a drastic improvement in performance as compared to conventional single-slice helical CT scanners could be achieved [14, 15]. Multidetector-row computed tomography has been validated as a useful non-invasive diagnostic method in patients with various cardiac diseases. Because of the combination of fast rotation time and multislice acquisition with a high spatial resolution, MDCT is able to provide detailed information on cardiac morphology and on the coronary arteries at the same time [16–18]. So far, only few scientific reports have been published regarding the detection of myocardial infarctions using MDCT. A recent systematic comparison between a four-slice MDCT scanner and contrast ventriculography [8] demonstrated promising diagnostic accuracies for the detection of recent as well as chronic myocardial infarctions when the authors employed a mixed criterion of hypo-attenuation and/or wall thinning. The reference test was, however, suboptimal because ventriculography relies on the presence of wall motion abnormalities that maybe absent even with significant degrees of MI [19].

MDCT myocardial perfusion imaging

Similarly to the scarce literature on CT imaging of myocardial infarctions, at present there is only little data available on the use of MDCT in myocardial perfusion imaging. Due to advantages in temporal resolution as well as volume coverage, electron-beam CT has been reported to be promising for the assessment of myocardial perfusion [20]. However, this scanner type is hardly used in clinical routine and only available in a limited number of centers worldwide. Animal studies using a combination of rest and stress perfusion scanning showed that differences in myocardial perfusion can be assessed using MDCT imaging [21, 22]. In addition it has been shown that a coronary perfusion reserve can be derived from MDCT data [23]. Wintersperger et al. [24] presented preliminary data of a small patient series showing reasonable results of absolute blood flow quantification using Fermi-function modeling. The main problem with MDCT myocardial perfusion imaging is that the scan protocol would have to be adapted to a stationary, volume-

covering dynamic acquisition, to assess the myocardial contrast uptake over time, similarly to MRI techniques [25]. However, this would result in a double exposure of the patient and additional amount of contrast agent needed. This type of perfusion scanning would not be suited for depiction of the coronary arteries, which is the most common contrast-enhanced cardiac application for MDCT these days and performed widely. In the study presented, we used a standard coronary angiography protocol optimized for a 16-slice CT, without the need of additional examination time, radiation exposure or contrast dose.

Discussion of results

As described above, decreased myocardial attenuation in contrast-enhanced MDCT using the routine, contrast-enhanced first-pass imaging protocol optimized for coronary artery imaging, may correspond to MI or to myocardial perfusion defects (but viable myocardium). A differentiation of these two entities without adaptation of the MDCT protocol seems difficult. That is why, in the present study, myocardial areas of hypo-attenuation in MDCT, possibly corresponding to myocardial perfusion deficits or myocardial infarctions, have been compared to both viability and perfusion imaging with MRI, applying stress-perfusion MRI as well as delayed-enhancement MRI as the standard of reference. Based on the presence of decreased X-ray attenuation, MDCT demonstrated high sensitivity (91%), specificity (79%) and diagnostic accuracy (83%) for the detection of MI. However, comparing MDCT to SP-MRI and only including the six patients with a true ischemic perfusion defect not corresponding to a MI, sensitivity was as low as 50%, while specificity was still as high as (92%). These findings indicate that myocardial areas of hypo-attenuation in MDCT can indeed correspond to infarctions and perfusion defects at the same time. As MDCT of the heart is typically performed at rest conditions (as it was in the study presented), sensitivity for perfusion defects detected with stress-perfusion MRI is significantly reduced. Retrospectively reviewing the MDCT data sets and separating areas of myocardial infarction and myocardial perfusion defects showed only few imaging findings that could help in the differentiation of these two entities. One imaging finding typical for myocardial infarctions might be abnormal wall thinning as compared to adjacent, viable myocardium, but this applies to chronic infarctions with scarring of the myocardium. A differentiation of recent infarctions with normal wall thickness and myocardial perfusion defects does not seem possible with the standard contrast-enhanced coronary angiography protocol. Here, application of delayed enhancement techniques might be useful. Applicability of such techniques using CT has been described earlier and has been reported to add significant information on the differential of viable vs non-viable myocardium [26]. However, this procedure requires a second delayed CT scan, increasing the radiation exposure of the patient.

Limitations

There are several limitations to the preliminary data presented in this study. All 11 myocardial infarctions present in the study population were chronic (i.e. older than 30 days), and sensitivity in the MDCT images for older infarctions is supposed to be higher than for recent infarctions, as it has been reported earlier [8]. However, current animal studies have reported promising diagnostic accuracies also in recent events [27]. Secondly, image analysis was performed subjectively and by only one investigator for each technique. Further studies will need to address the issue of reproducibility, and possibly introduce a way of quantitative data analysis. A threshold value of myocardial attenuation may be useful to objectively differentiate infarcted and viable segments. However, the results of this study show significant overlap in HU between the two types of tissue and additionally, as we have demonstrated, an area of hypoattenuation may correspond to necrotic as well as viable (hypoperfused) myocardium. Finally, myocardial perfusion defects as detected in MDCT, performed at resting conditions, were compared to MRI stress perfusion data. The reason for this approach was to test MDCT in the assessment of perfusion defects versus a reference standard technique with a high diagnostic accuracy.

Conclusions

In addition to detailed information on the coronary artery tree, contrast-enhanced 16-detector row CT of the heart provides valuable information on myocardial viability and perfusion without an increase in volume of contrast agent or radiation dose administered to the patient. Sensitivity for chronic MI is high, and infarct volume and localization correlate well to findings in delayed-enhancement MRI. However, diagnostic accuracy for the assessment of myocardial perfusion defects is reduced comparing MDCT data to stress-perfusion MRI, most probably because contrast-enhanced MDCT of the heart is typically performed at resting conditions. Finally, a differentiation of these two entities (MI versus hypoperfusion) without adaptation of the MDCT protocol seems difficult.

References

1. Sabharwal NK, Lahiri A (2003) Role of myocardial perfusion imaging for risk stratification in suspected or known coronary artery disease. Heart 89 (11):1291–1297
2. Kannel WB, Abbott RD (1984) Incidence and prognosis of unrecognized myocardial infarction. An update on the Framingham study. N Engl J Med 311 (18):1144–1147
3. Constantine G, Shan K, Flamm SD, Sivananthan MU (2004) Role of MRI in clinical cardiology. Lancet 363 (9427):2162–2171
4. Kim RJ, Fieno DS, Parrish TB, Harris K, Chen EL, Simonetti O et al. (1999) Relationship of MRI delayed contrast enhancement to irreversible injury, infarct age, and contractile function. Circulation 100(19):1992–2002
5. Paetsch I, Jahnke C, Wahl A, Gebker R, Neuss M, Fleck E et al. (2004) Comparison of dobutamine stress magnetic resonance, adenosine stress magnetic resonance, and adenosine stress magnetic resonance perfusion. Circulation 110(7):835–842
6. Barkhausen J, Hunold P, Jochims M, Debatin JF (2004) Imaging of myocardial perfusion with magnetic resonance. J Magn Reson Imaging 19(6):750–757
7. Nikolaou K, Poon M, Sirol M, Becker CR, Fayad ZA (2003) Complementary results of computed tomography and magnetic resonance imaging of the heart and coronary arteries: a review and future outlook. Cardiol Clin 21 (4):639–655
8. Nikolaou K, Knez A, Sagmeister S, Wintersperger BJ, Reiser MF, Becker CR (2004) Assessment of myocardial infarctions using multirow-detector computed tomography. J Comput Assist Tomogr 28(2):286–292
9. Kellman P, Arai AE, McVeigh ER, Aletras AH (2002) Phase-sensitive inversion recovery for detecting myocardial infarction using gadolinium-delayed hyperenhancement. Magn Reson Med 47(2):372–383
10. Huber DJ, Lapray JF, Hessel SJ (1981) In vivo evaluation of experimental myocardial infarcts by ungated computed tomography. Am J Roentgenol 136(3):469–473
11. Slutsky RA, Peck WW, Mancini GB, Mattrey RF, Higgins CB (1984) Myocardial infarct size determined by computed transmission tomography in canine infarcts of various ages and in the presence of coronary reperfusion. J Am Coll Cardiol 3(1):138–142
12. Schmermund A, Gerber T, Behrenbeck T, Reed JE, Sheedy PF, Christian TF et al. (1998) Measurement of myocardial infarct size by electron beam computed tomography: a comparison with 99 mTc sestamibi. Invest Radiol 33(6):313–321
13. Georgiou D, Bleiweis M, Brundage BH (1992) Conventional and ultrafast computed tomography in the detection of viable versus infarcted myocardium. Am J Card Imaging 6(3):228–236
14. Ohnesorge B, Flohr T, Becker C, Kopp AF, Schoepf UJ, Baum U et al. (2000) Cardiac imaging by means of electrocardiographically gated multisection spiral CT: initial experience. Radiology 217(2):564–571
15. Kopp AF, Kuettner A et al. (2003) MDCT: cardiology indications. Eur Radiol 13(Suppl 5):M102–M115
16. Becker CR, Knez A, Leber A, Treede H, Ohnesorge B, Schoepf UJ et al. (2002) Detection of coronary artery stenoses with multislice helical CT angiography. J Comput Assist Tomogr 26(5):750–755
17. Nieman K, Cademartiri F, Lemos P, Raaijmakers R, Pattynama P, de Feyter P (2002) Reliable noninvasive coronary aniography with fast submillimeter multislice spiral computed tomography. Circulation 106:2051–2054
18. Achenbach S, Giesler T, Ropers D, Ulzheimer S, Derlien H, Schulte C et al. (2001) Detection of coronary artery stenoses by contrast-enhanced, retrospectively electrocardiographically-gated, multislice spiral computed tomography. Circulation 103 (21):2535–2538
19. Mahrholdt H, Wagner A, Parker M, Regenfus M, Fieno DS, Bonow RO et al. (2003) Relationship of contractile function to transmural extent of infarction in patients with chronic coronary artery disease. J Am Coll Cardiol 42 (3):505–512
20. Georgiou D, Wolfkiel C, Brundage BH (1994) Ultrafast computed tomography for the physiological evaluation of myocardial perfusion. Am J Card Imaging 8(2):151–158
21. So A, Hadway J, Pan T, Lee TY (2002) Quantitative myocardial perfusion measurement with CT scanning. Radiology 225:308
22. Stantz KM, Liang Y, Meyer CA, Teague SD, March K (2002) In vivo myocardial perfusion measurements by ECG-gated multi-slice computed tomography. Radiology 225:308
23. Hadway J, Sykes J, Kong H, Lee TY (2003) Coronary perfusion reserve as measured by CT perfusion. Radiology 229:305
24. Wintersperger BJ, Ruff J, Becker CR, Knez A, Huber A, Nikolaou K (2002) Assessment of regional myocardial perfusion using multirow-detector computed tomography. Eur Radiol 12 (Suppl I):294
25. Chiu CW, So NM, Lam WW, Chan KY, Sanderson JE (2003) Combined first-pass perfusion and viability study at MR imaging in patients with non-ST segment-elevation acute coronary syndromes: feasibility study. Radiology 226(3):717–722
26. Koyama Y, Mochizuki T, Higaki J (2004) Computed tomography assessment of myocardial perfusion, viability, and function. J Magn Reson Imaging 19(6):800–815
27. Hoffmann U, Millea R, Enzweiler C, Ferencik M, Gulick S, Titus J et al. (2004) Acute myocardial infarction: contrast-enhanced multi-detector row CT in a porcine model. Radiology 231 (3):697–701